



# Quinoline derivatives strategically designed. Estimation of its antioxidant and neuroprotective activity.

Luis Felipe Hernandez-Ayala,<sup>1</sup> Eduardo Gabriel Guzmán-López,<sup>1</sup> and Annia Galano<sup>1,\*</sup>

<sup>1</sup> Departamento de Química, Universidad Autónoma Metropolitana-Iztapalapa, Av. Ferrocarril San Rafael Atlixco 186, Col. Leyes de Reforma 1A Sección, Alcaldía Iztapalapa, Mexico City 09310, Mexico.\*

**Abstract:** Quinoline has been proposed as a privileged molecular framework in medicinal chemistry. Although by itself it has very few applications, its derivatives have diverse biological activities. In this work, 8536 quinoline derivatives strategically designed using the CADMA-Chem protocol are presented. This large chemical space was sampled, analyzed and reduced using selection and elimination scores that combine their properties of bioavailability, toxicity and manufacturability. After applying the above filters, 25 derivatives were selected to investigate their acid-base, antioxidant and neuroprotective properties. The antioxidant activity was predicted based on the ionization potential and bond dissociation energies, parameters directly related to the transfer of hydrogen atoms and of a single electron, respectively. These two mechanisms are typical in the radical scavenging process. The antioxidant efficiency was compared with reference compounds and the most promising antioxidants were found to be more efficient than Trolox but less efficient than ascorbate. In addition, based on molecular docking simulations, some derivatives are expected to act as inhibitors of catechol-O methyltransferase (COMT), acetylcholinesterase (AChE) and monoamine oxidase type B (MAO-B) enzymes. Some structural insights about the compounds were found, these can enhance or decrease the neuroprotection activity. Based on the results, four quinoline derivatives are proposed as candidates to act as multifunctional antioxidants against Alzheimer's (AD) and Parkinson's (PD) diseases.

**Keywords:** Rational design, quinoline derivatives, antioxidants, neuroprotection, Alzheimer and Parkinson diseases.

## 1. Introduction

In an oxidative stress (OS) condition, there is an excess of pro-oxidants that cannot be counteracted by the antioxidant systems [1]. Under pathological situation, there is a state of chronic OS where cellular metabolism increases the production of free radicals and reactive oxygen species (ROS) [2-5]. The brain consumes large amounts of oxygen to carry out its physiological functions, and therefore generates a high number of free radicals. Some factors make the brain susceptible to ROS attack, such as the lack of antioxidant mechanisms, its particularly rich fatty acid composition [6], and the low permeability of the blood-brain barrier [7-9], which reduces the passage of many antioxidants such as vitamin E. Due to this, OS has been studied mainly in neurodegenerative diseases such as Alzheimer's disease (AD), Parkinson's disease (PD), among others [10,11]. OS situations have been observed in these diseases, even in early stages, indicating that ROS and other free radicals could be related to their etiology [12,13].

Several lines of research have implicated the OS and free radical damage in the origin and pathogenesis of AD [12,14-17]. This damage includes energy metabolism and overcompensation of antioxidant enzymes [17]. Despite the extensive literature regarding OS in AD, the sources of increased free radicals responsible for initiating such damage remain unclear. However, some candidates could be activated microglia [18],  $\beta$ -amyloid protein deposits [19], modified lipoxidation advanced proteins [20] and the increase in the concentration of metals such as iron and copper [21-25]. In the case of PD, evidence suggests

**Citation:** To be added by editorial staff during production.

Academic Editor: Firstname Last-name

Received: date

Revised: date

Accepted: date

Published: date

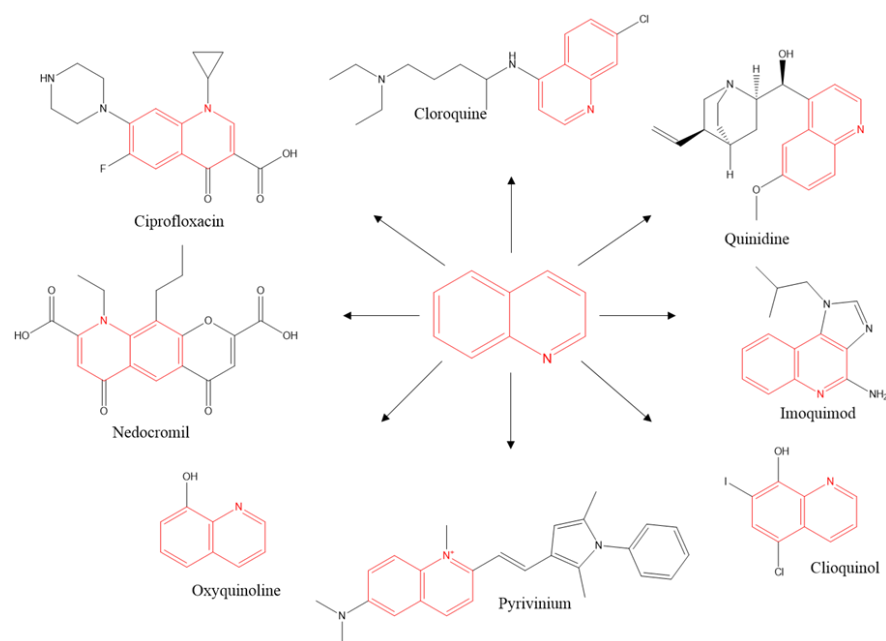


**Copyright:** © 2023 by the authors. Submitted for possible open access publication under the terms and conditions of the Creative Commons Attribution (CC BY) license (<https://creativecommons.org/licenses/by/4.0/>).

that deficiencies in mitochondrial function, increased oxidative stress, apoptosis and inflammation [26-29] are part of the processes that eventually result in neurodegeneration. Also, the ROS generated by the oxidation of dopamine have been implicated in the destruction of neurons related to age and other neurodegenerative processes such as PD [30-32]. Two enzymes are involved in the dopamine oxidation process, monoamine oxidase (MAO) and catechol-O-methyl transferase (COMT), whose reactions produce considerable quantities of superoxide and hydroxyl radicals, as well as hydrogen peroxide [33-35].

Quinolines are aromatic heterocycles formed by the fusion of a benzene nucleus with a pyridine ring. Quinoline as such has few applications, but it is considered a privileged structure [36-40] from which derivatives are built that are useful in various fields [41-44], mainly medicinal chemistry. A prominent example of these derivatives is quinine, an alkaloid found in plants that has long been the main choice in the treatment of malaria [45]. More than 200 biologically active quinoline alkaloids have been identified [46]. The primary use of this compound is as a precursor to 8-hydroxyquinoline, a versatile chelating agent and pesticide precursor [47]. The interest to study the quinoline derivatives has increased since these are of great importance for the pharmaceutical industry. This interest has driven the development of simple and eco-friendly synthesis methods that represents an advantage over other molecular scaffolds [48-52].

The large literature on the synthesis of quinoline and its derivatives has encouraged researchers to explore this molecular framework for potential drugs. Quinoline is a characteristic structural motif of many drugs used in the clinic for the treatment of various diseases, its main application being antimalarial drugs [18]. Since heterocyclic molecules are used as the set of bases for drug discovery and development, the quinoline ring is a framework with different advantages and representing a wide variety of potential benefits. Its derivatives have been studied as possible antibacterial, antifungal, antimycobacterial, antiviral, antiprotozoal, antimalarial, anticarcinogenic, antioxidant, anticonvulsant, analgesic, anti-inflammatory, anthelmintic agents, as well as beneficial against diseases of the nervous system such as cardiovascular and other biological activities [53-70]. In the Scheme 1 are presented some quinoline contain approved drugs.



**Scheme 1.** Quinoline approved drugs

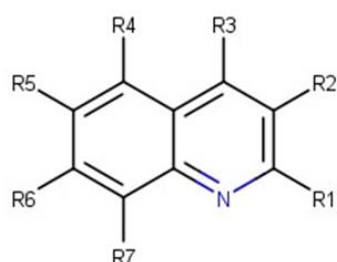
A strategical, systematic, and rational search for quinoline derivatives with antioxidant and neuroprotector activities has been performed using the CADMA-Chem protocol

[71]. Bioavailability, toxicity, synthetic availability, electron, and hydrogen atom donating capabilities, and the potential for inhibiting COMT, AChE, and MAO-B enzymes were explored. According to the obtained results, the promising candidates were identified and proposed for further investigations.

## 2. Materials and Methods

### 2.1. Construction of derivatives and estimation of molecular properties.

Quinoline derivatives (Q1, Scheme 2) were systematically designed. For this, Smile-it tool was used, it was developed in the working group of the research team and is available at (<https://agalano.com/Smile-It/>). The seven possible sites of the scaffold were substituted. The mono, di, and tri-substituted compounds with six functional groups (-OH, -NH<sub>2</sub>, -SH, -COH, -COCH<sub>3</sub> and -COOCH<sub>3</sub>) were analyzed. According to this, 8356 dQ derivatives were designed.



**Scheme 2.** Quinoline (R1-R7=H) and their derivatives (dQ)

For all the derivatives designed, the parameters of absorption, distribution, metabolism and excretion (ADME) were estimated with the open source chemoinformatics tools RDKit [72]. These parameters were used to confirm whether the derivatives satisfy the rules of Lipinski, Ghose, Veber, Egan and Muegge [73-77]. Compounds that violate more than one of these rules have difficulties with bioavailability and could present permeation problems. Its difficulty of synthesis was also evaluated by means of the synthetic accessibility (SA) parameter calculated with the AMBIT-SA software specialized in organic molecules [78]. A value between 0 and 100 is estimated. The higher the value, the easier the compound is to synthesize. The safety of the compounds was estimated by four parameters, using the Toxicity Estimation Computer Tool (T.E.S.T.), version 5.1.2 [79]. Rodent median lethal dose (LD<sub>50</sub>), Ames mutagenicity (M), developmental toxicity (DT), and bioaccumulation factor (BF) were used to assess the toxicity of quinoline and its derivatives. The significance of each parameter and the criteria used is defined in Table S1.

To select samples from the constructed chemical space, selection and elimination scores were used as expressed in terms of the parameters described above [80,81]. For comparison purposes, a set of reference molecules was used, which have been used as neuroprotectors or are being investigated in advanced clinical phases with this same activity (Table S2).

### 2.2. DFT calculations.

Electronic structure calculations were performed with density functional theory (DFT) using Gaussian 16 [82] software. Geometric optimizations and frequency calculations were performed using a M05-2X/6-311+G(d,p) protocol, no imaginary frequencies were obtained, ensuring that the structures are minimal on the potential energy surface. Solvation effects were simulated using the universal solvation model (SMD) [83], using water as solvent. M05-2X has popular functionalities for various databases and its performance in various difficult cases is accurate. The tests include barrier heights, conformational energy and the trend in bond dissociation energies [84], it is recommended to model

open shell systems [84]. This functional has been successfully used to determine the bond dissociation energies (BDE) and the radical scavenging capacity of several antioxidants [85–89].

Electron propagator theory (EPT)[90] was used to calculate ionization energies (IE). For the estimation of BDE, all the probable sites for the donation of H atoms were considered, that is, the  $-CH_3$  in the quinoline ester fraction, and the phenolic OH in the different functionalization sites, from R1 to R7 (Scheme 1).

Deprotonation route was predicted with Marvin suite [91] and the pKa values were refined with DFT fitted parameters procedure [92]. This property is of crucial importance for medical drugs since it governs the proportion of neutral species at a particular pH, and these are the species most likely to passively cross biological barriers. This method of prediction and calculation of pKa values has been tested before, offering results comparable to those reported experimentally [93].

### 2.3. Protein-ligand docking details.

The structures of enzymes were obtained from protein data bank. The data are summarized in the Table 1.

**Table 1.** Data of proteins used in the docking simulations.

Enzyme	Co-crystallized inhibitor	Substrate
COMT	Tolcapone [94]	Dopamine
MAOB	Safinamide [95]	Phenylethylamine
AChE	Donepezil [96]	Acetylcholine

AChE misplaced loop regions (256–261 and 493–496 residues) were fixed using Modeller [97]. Water and solvent molecules, chloride ions and non-relevant species were removed with Autodock Tools [98]. Protein ionizable residues were considered at physiological pH, i. e., the protonation state of lateral chains for D, E were considered as deprotonated species and R, K and H as protonated amino acids. For quinolines, natural substrates and inhibitors atomic charges estimated by NBO protocol with DFT (M05-2X/6-311+G(d,p)) methodology. Docking simulations were carried out using AutoDock Vina 1.2.0 software [99]. A gradient optimization algorithm was performed inside of the active site centered at x: -13.50, y: 37.69, z: 61.63 and grid size of 15 x 15 x 15 Å<sup>3</sup> for COMT, x: 51.81, y: 156.34, z: 28.15 and grid size of 15 x 15 x 15 Å<sup>3</sup> for MAO-B and x: -16.30, y: -43.83, z: 30.17 and grid size of 21 x 21 x 21 Å<sup>3</sup> for AChE. Docking scores ( $\Delta G_B$ ) were reported for the best docked pose and then this score was weighted according to the fractions of each relevant specie at pH= .4. For the five most stable complexes, the conformation protein-ligand was analyzed and drawn with Discovery Studio software [100]. Redocking simulations were carried out and the RMSD values for inhibitors 1.8, 1.6 and 2.8 Å and the scores 7.6, 10.0 and 12.0 kcal/mol were founded for tolcapone, safinamide and donepezil respectively, agrees with experimental IC<sub>50</sub>, Ki or  $\Delta G_B$  findings [95,96,101]. These results confirm the suitability of our docking methodology.

## 3. Results and discussion

### 3.1. Screening the chemical space. Selection and elimination scores

Due to the substitution of -OH, -NH<sub>2</sub>, -SH, -COH, -COCH<sub>3</sub> and -COOCH<sub>3</sub> groups in the R1 to R7 sites and the study the mono-, di- and tri-substituted compounds 8359 quinoline derivatives were built. Forty-two of them are monosubstituted compound, seven hundred fifty-six are disubstituted and seven thousand five hundred sixty are trisubstituted compounds. Since some toxicity values for 2033 derivatives could not be estimated, they were eliminated in a first screening. All designed compounds investigated were reported in the supporting information file 1 (SIF1.pdf).

The selection score (SS) was the indicator applied to sample the generated chemical space. The values obtained for this selection parameter oscillate between 2.36 and 3.54. The selection score considers the bioavailability of the compounds through the estimation of the ADME properties, it also contemplates the toxicity and the ease with which the compounds should be synthesized. According to the values obtained, the derivatives that beat the performance of the parent molecule (SS=2.83) and the average of the reference set (SS=3.00) are five hundred and thirty compounds.

This scoring system considers the averages of the variables (ADME, toxicity, and synthetic accessibility) and may mask flaws in some property. To overcome this obstacle, an elimination function (SE) was developed that indicates the deviations of the values of each property with respect to the reference set. This function can be analyzed as a whole or by individual property, which is more useful. Furthermore, SE works as an additional filter to choose the most promising derivatives. The elimination function contains all deviations from each property and is a sum of the individual elimination coefficients. The details about the SS and SE calculations can be founded in the supporting information.

Using this exclusion score, further evaluation was achieved. At this point, 25 derivatives were chosen. The structures of the best-scoring derivatives and the molecular framework (dQ1) are presented in Figure 1.

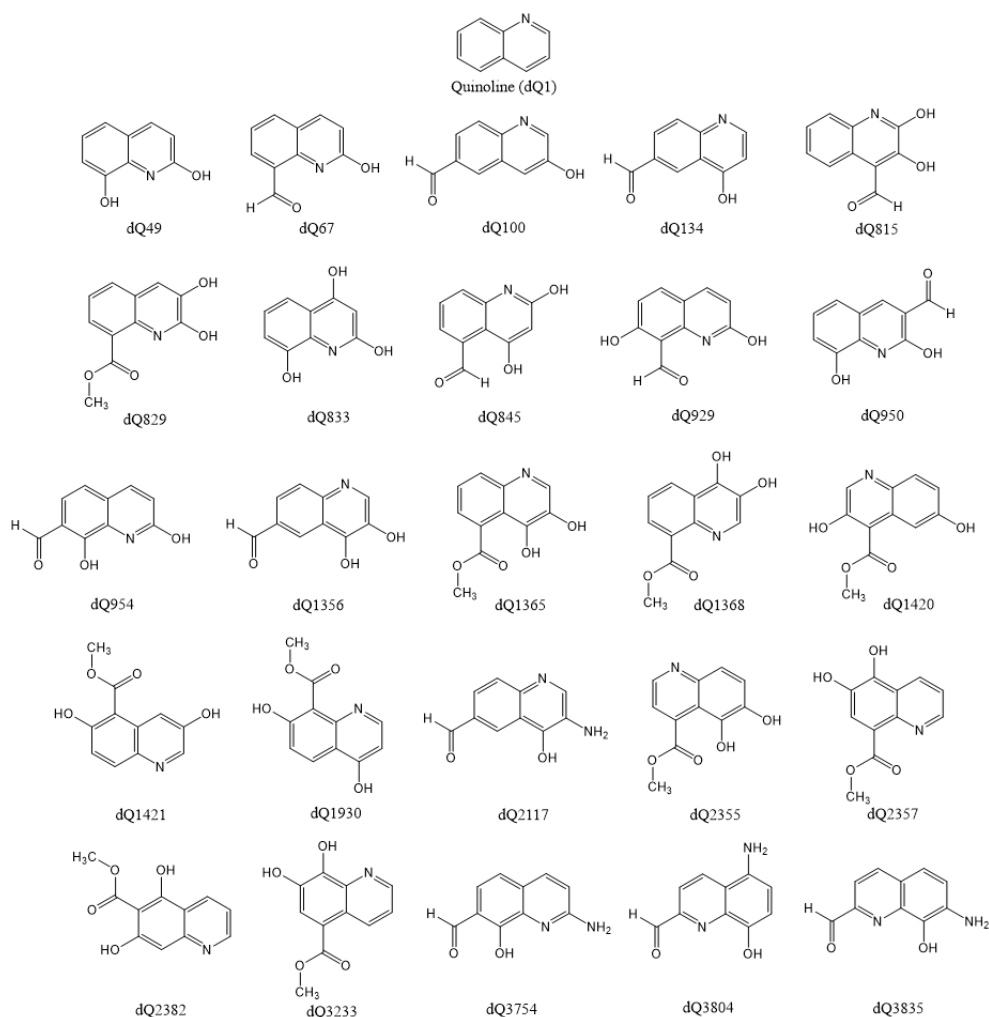


**Figure 1.** 2D Structures of the best scored (SS y SE) quinoline derivatives.

Due to the large number of studied compounds, only the  $S^S$  and  $S^E$  plots (in Figures 2 and 3 respectively) are presented for the twenty-five most promising derivatives.

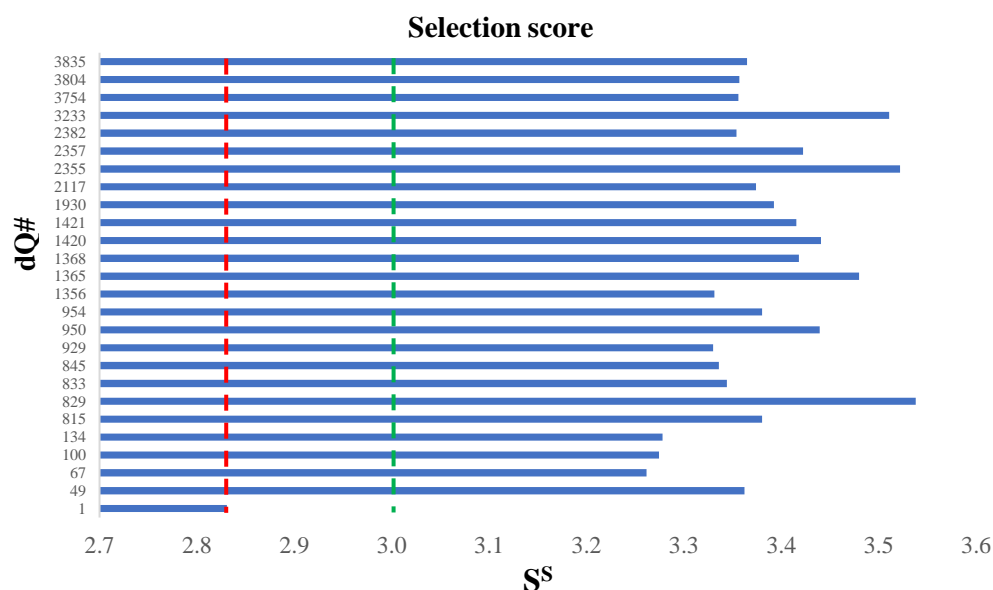


**Figure 2.** Selection score SS for the best quinoline derivatives. Red line is the estimated value for quinoline scaffold and green line represents the average selection score for reference set.

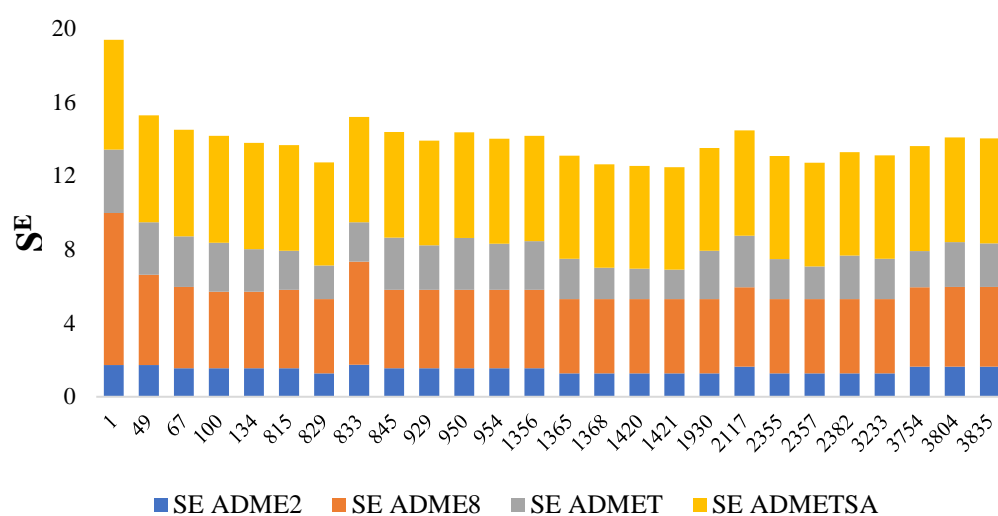


**Figure 3.** Elimination score ( $S^E$ ) by set of properties for the most promising quinoline derivatives. The size of the segments represents the deviations from the estimated values for the reference set.

In general, molecules with higher  $S^S$  values are expected to have lower toxicity, easier synthesis, and better bioavailability, i.e., they would have all the desirable aspects for a good oral drug. In the case of  $S^E$ , the values ranging from 12.5 to 19.4, the highest value being that obtained for the parent molecule. In the Figure 3, are presented the plot of  $S^E$  values for a set of properties, SADME2, SADME8, SADMET and SADMETSA. These plot show that the major deviations (with respect to the reference set) are the ADME properties and the synthetic accessibility. In the first case the ADME properties presents a negative variation since the derivatives are significantly smaller that the reference set molecules. On the other hand, the synthetic accessibility of our derivatives represents a serious advantage is an advantage over the recognized neuroprotectors. Finally, this plot is not enough to analyze the deviations of toxicity parameters, to analyze that an individual contribution plot are presents in the Figure 4.

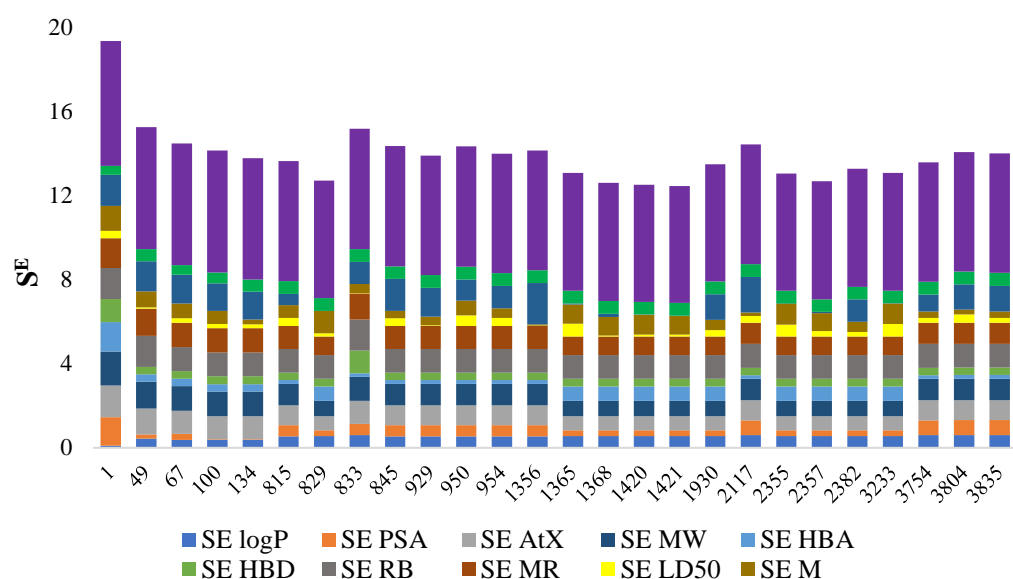


**Figure 4.** Individual contributions to the elimination score (SE) for the most promising quinoline derivatives.

Except for quinoline, all the derivatives present a slightly higher LD50 (yellow segment), the same case occurs with mutagenicity (gold segment) but the deviation is more pronounced. For all derivatives, the bioaccumulation factor (light green bar) is lower than the average of the reference set, however this parameter shows a very large dispersion in these compounds, which makes this elimination score small. The most significant case is developmental toxicity (aqua bar), quinoline and its derivatives are less toxic than the reference set, in some cases the deviation is remarkable, such as compounds dq845, dQ1356 and dQ2117. Since the twenty-five compounds have acceptable bioavailability (no violations of the Lopinski, Egan, Muegge, Ghose and Veber rules), low toxicity and easier manufacturability (than the reference set), all compounds were kept in the next stage of the investigation to evaluate their potential antioxidant and neuroprotective activity.

### 3.2. Acid-base equilibria and antioxidant activity.

In potential drugs, the study of the acid-base balance is crucial to find out if the molecules can cross biological barriers by passive diffusion. Deprotonation pathways and estimated pka values are found in Figure S1. Molar fractions (represented as percentage X%) at biological pH are found in Table 2.

In most of the compounds the neutral species (X%dQ) predominates at pH=7.4, however, there are several derivatives that present an important anionic fraction (X%H-1dQ-), in the case of dQ833 and dQ2382, the cationic species (X%HdQ+) has a significant percentage (>1.0%) and for dQ1421 the dianionic form has a little amount. Among the analyzed derivatives dQ829, dQ833, dQ954, dQ1365, dQ1368, dQ1930, dQ2355, dQ2357 have an important amount of both neutral and anionic species. According to the portion of neutral form, these compounds should not present problems to cross the barriers passively and additionally, and according to the group's experience, the antioxidant activity can be enriched by the presence of a significant amount of the charged species.

**Table 2.** Estimated percentage fractions of the dQ acid-base species at pH= 7.4

dQ	X% $\text{H}_2\text{dQ}^{2+}$	X% $\text{HdQ}^+$	X% $\text{dQ}$	X% $\text{H}_1\text{dQ}^-$	X% $\text{H}_2\text{dQ}^{2-}$	X% $\text{H}_3\text{dQ}^{3-}$
1	---	0.0	100.0	---	---	---
49	---	0.0	79.6	29.4	0.0	---
67	---	0.0	98.7	1.3	---	---
100	---	0.0	84.9	15.1	---	---
134	---	0.0	100.0	0.0	---	---
815	---	0.0	92.4	7.6	0.0	---
829	---	0.0	30.9	69.1	0.0	---
833	---	1.1	63.3	35.6	0.0	0.0
845	---	0.0	98.7	1.3	0.0	---
929	---	0.0	88.6	11.4	0.0	---
950	---	0.0	98.8	1.2	0.0	---
954	---	0.0	59.7	40.3	0.0	---
1356	---	0.0	97.7	2.3	0.0	---
1365	---	0.0	68.1	31.2	0.0	---
1368	---	0.0	31.4	68.6	0.0	---
1420	---	0.3	28.4	71.3	0.0	---
1421	---	0.1	80.1	18.8	1.0	---
1930	---	0.0	56.8	43.2	0.0	---
2117	---	0.1	99.9	0.0	---	---
2355	---	0.0	56.3	43.7	0.0	---
2357	---	0.0	68.6	31.4	0.0	---
2382	---	4.3	92.8	2.9	---	---
3233	---	0.1	54.0	46.0	---	---
3754	---	0.0	98.0	2.0	---	---
3804	0.0	0.0	98.0	2.0	---	---
3835	0.0	0.0	98.8	1.2	---	---

Ionization potential (IP) and bond dissociation energies (BDE) were calculated for the acid-base species with non-negligible fraction ( $X\%dQ \geq 1\%$ ), the whole results are presented in the Table S3. The sp<sup>3</sup> hydrogens were considered as potential H-donating sites, i.e., phenol, amine and methyl groups, in this order, quinoline was not considered since it does not contain H-atoms like those mentioned above. BDE and IP are related with the capability of the compounds to the donate H-atoms and electron respectively. Then, these parameters were used to evaluate the efficacy of the ascorbate derivatives as free radical scavengers via single electron transfer (SET) and hydrogen atom transfer mechanisms (HAT), respectively, comparing them with some reference antioxidants such as Trolox,  $\alpha$ -tocopherol and ascorbate and with the latent oxidant target  $\text{H}_2\text{O}_2/\bullet\text{OOH}$ . To analyze the scavenging efficiency, the electron and hydrogen atom donation map for antioxidants (eH-DAMA) was constructed with IP and BDE, this map is presented in the Figure 5.

According to the eH-DAMA, anionic species are the most efficient. Almost all compounds will be capable of scavenging hydroxyl radicals, likewise most species are more efficient than  $\alpha$ -tocopherol. The most powerful antioxidants are those with a greater antioxidant potential than Trolox, among them are derivatives dQ49, dQ829, dQ950, dQ1356, dQ1368, dQ2355 and dQ2357. dQ49 has better H-atom dative behavior than Trolox and is

248

249

250

251

252

253

254

255

256

257

258

259

260

261

262

263

264

265



as strong an electron donor as this antioxidant. The results suggest that the remaining compounds would be better radical scavengers via both SET and HAT mechanisms than Trolox. Finally, five compounds have better radical scavenging performance via the HAT mechanism than ascorbate (vit. C) but are less efficient via the SET mechanism. At this point it is worth noting that vitamin C is one of the antioxidants present in the biological environment [102].

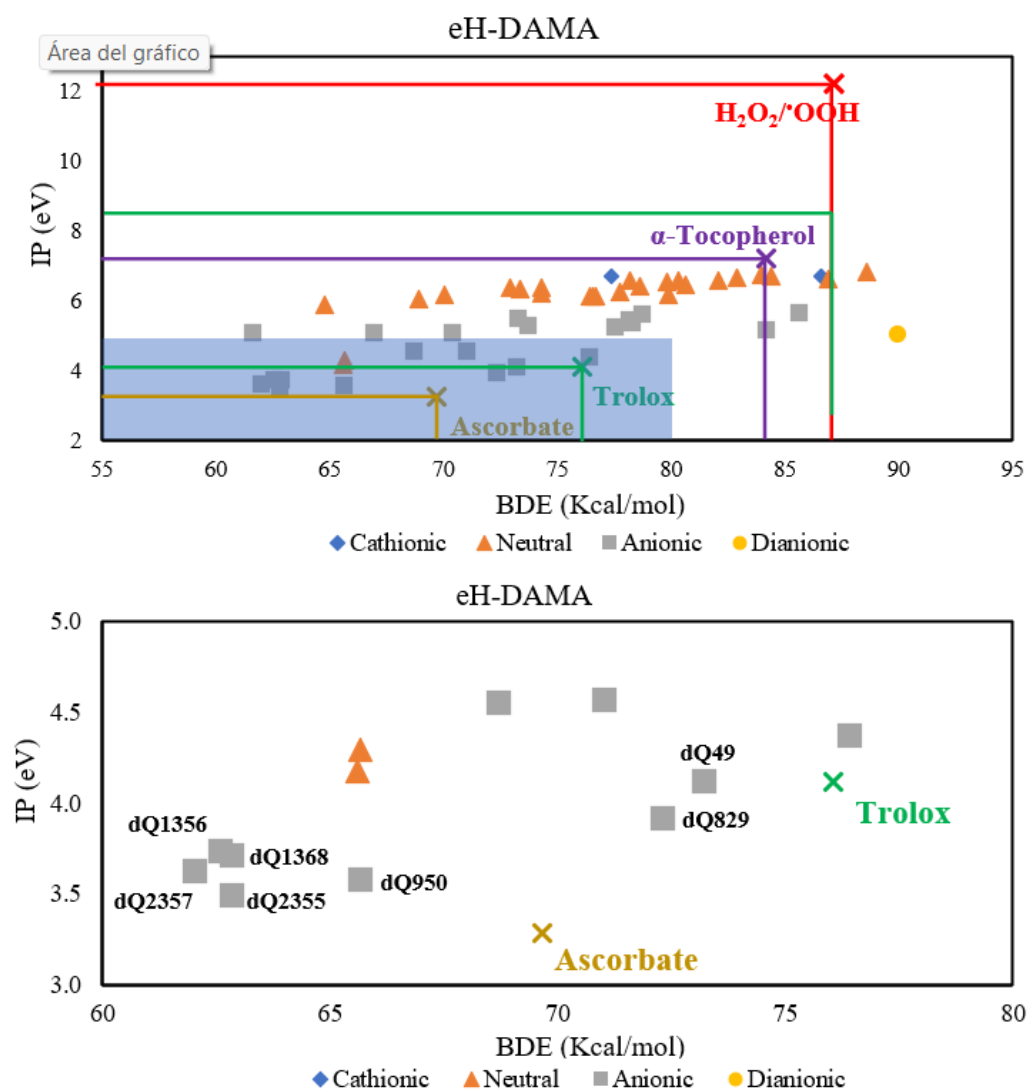


**Figure 5.** The electron and hydrogen donating ability map for antioxidants (eH-DAMA) for the most promised compounds and their significant species at physiological pH (top). Some typical antioxidants are presented as comparison. Close up to the most promised antioxidants (bottom).

### 3.3. Neuroprotection assessment.

To assess the neuroprotective activity of quinoline derivatives, the weighted docking scores and polygenic score (SP) of the most promised candidates were reported in the Table 4. The complete set of docking data are in the Table S4. SP is a measure of the affinity of compounds towards enzymes compared to their natural substrates dopamine (COMT), dopamine, phenylethylamine (MAOB) and acetylcholine (AChE) and is defined based on our previous reports [93].

Based on the docking data, quinoline presents less affinity than the natural substrates of COMT and AChE, this is the origin of its lower SP value. As with other properties it seems

that the molecular framework by itself lacks chemical or biological interest, they are the functionalized derivatives that present the neuroprotective activity. The SP values suggest that the compounds exhibit neuroprotective activity since the score is magnitude higher than the natural substrates, in a general view, the quinoline derivatives have a good affinity with the enzymes and could inhibit its natural function. Among the compounds studied, it was the analogue dQ929 in which the best neuroprotective efficiency was observed.

**Table 4.** Scoring values of quinoline derivatives

dQ	$\Delta G_{B^W}$ (kcal/mol)			S <sup>P</sup>
	COMT	MAO-B	AChE	
Quinoline	-5.00	-6.90	-3.80	2.85
49	-6.00	-8.34	-8.20	4.18
815	-6.26	-7.91	-9.02	4.11
829	-6.80	-8.41	-8.74	4.44
954	-5.78	-8.16	-8.24	4.11
1368	-5.96	-8.07	-8.24	4.13
2357	-6.29	-8.06	-7.93	4.13

$\Delta G_{B, \text{dopamine}} = -5.4$  kcal/mol in COMT;  $\Delta G_{B, \text{phenylethylamine}} = -6.0$  kcal/mol in MAO-B;  $\Delta G_{B, \text{acetylcholine}} = 4.9$  kcal/mol in AChE. For natural substrates S<sup>P</sup>=3.00

Although most of the compounds presented enhanced S<sup>P</sup> values, analysis of individual affinity values can reveal interesting data on the behavior of protein-ligand complexes that can be formed. For this we have designed the polygenic score plot (PSP) found in Figure 6. The colored fragments indicate the affinity for the respective protein and are calculated as the logarithm, the greater the length of the bar, the greater the affinity the compound will present for the enzyme. On the contrary, if it has a negative magnitude, it means that it does not present neuroprotective activity.

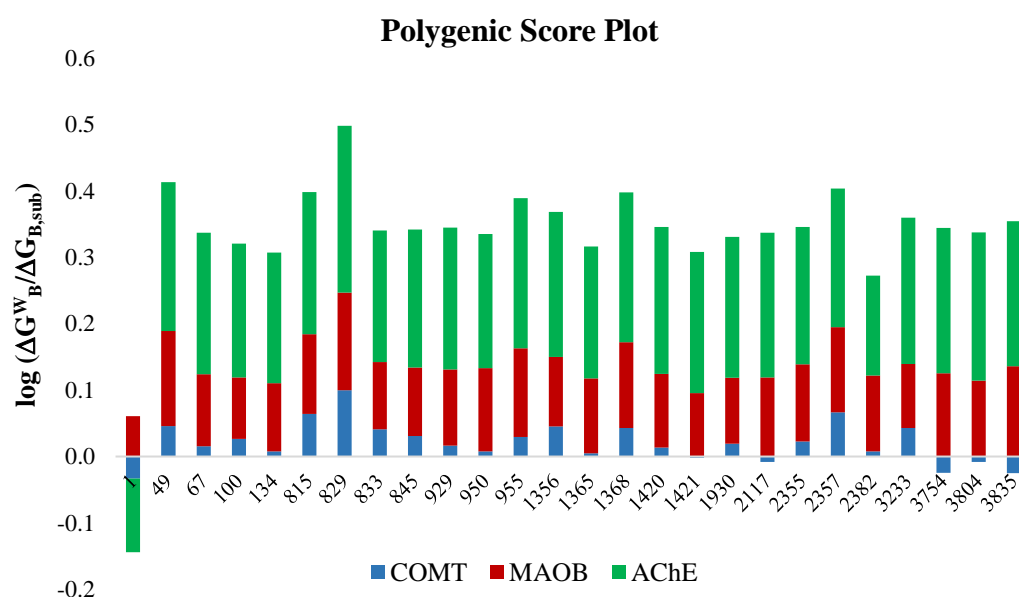


**Figure 6.** Polygenic score (SP) for the most promised quinoline derivatives. Green bars correspond individual scores.

According to the data in the graph, quinoline derivatives could preferentially inhibit the action of AChE and MAOB enzymes (red and green fragments respectively). In the case of COMT (blue fragments) the behavior of the compounds is heterogeneous, there are compounds that can inhibit the enzyme well (dQ829 and dQ2357), while others have practically the same affinity value as dopamine (dQ950 and dQ1421,  $\log=0$ ) and others that have no protective activity (dQ2117, dQ3754, dQ3804, dQ3835). Interestingly, and contrary to what would be expected, it seems that the amino groups do not favor binding to the receptor, since all tested amino compounds presented negative magnitudes. A possible explanation for this observation is that, unlike the substrate, the amino groups of the quinoline derivatives are directly attached to the aromatic rings, whereas in dopamine this group is attached to more accessible and flexible aliphatic chain. On the other hand, the large length of the AChE and MAOB fragments indicate a better activity against the degradation of phenylethylamine and acetylcholine, respectively. Regarding the groups that seem to favor the affinity for the enzyme, there are the aldehyde and ester carbonyl groups, since five of the 6 compounds with the highest affinity present this type of groups. In the case of AChE, the explanation could be the recognition of these groups, since it is in the hydrolysis of esters is the highly specialized function of these enzymes [103]. In the case of MAOB, it would be the great hydrophobic environment of the active site, rich in aromatic amino acids, which would promote the stability of the complex. This would explain the activity of the molecular framework since it was the only enzyme in which it presented considerable neuroprotective activity, presumably because of the hydrophobic interactions it can generate.

In the top of the Figure 7 is presented de 3D diagram of the stabilizing interactions in the complex formed between of the dQ829 with AChE. In the left-bottom of this figure, also can be observed a 2D map that describes in a better way this interaction path. Several H-bonds are originated by the hydroxyl and carboxyl-ester groups and the residues of the pocket of the protein, some of them with key amino acids of ethe active site. The ester moiety was in the anionic site of the enzyme, interacting with Gly121 and Gly122 via two H-bonds at the carbonyl oxygen. This same group seems to mimic the acetylcholine binding, forming an unfavorable bump interaction, blocking catalytic site (Ser203-Glu-Hys447). On the other hand, one of the hydroxyl groups is joined by another H-bond with the residue Tyr124 in the peripheral site. The Trp86 of the acyl site are binding via  $\pi$ -stacking interactions, remaining a recognized reversible AChE inhibitor tacrine [104], which, by the way, has a similar structure to quinoline. Due to this form of interaction, the compound appears to be a pseudo-reversible inhibitor of the AChE enzyme.

The 2D interaction diagram between MAO-B and dQ829 are in the bottom-middle of the Figure 7. The stabilizing interactions of the adduct formed are of a diverse nature. This is reasonable considering the versatility of functional groups that this quinoline derivative contains. Among the most important interactions are those formed between the derivative with the tyrosine fragments, most of them of hydrophobic nature. These residues have a critical role in the maintenance of stable and active conformation of the protein [105]. Likewise, the union of dQ829 with the FAD fragment, via  $\pi$ -forces, would effectively inhibit the action of MAOB, since this is responsible for the oxidation of amines [106].

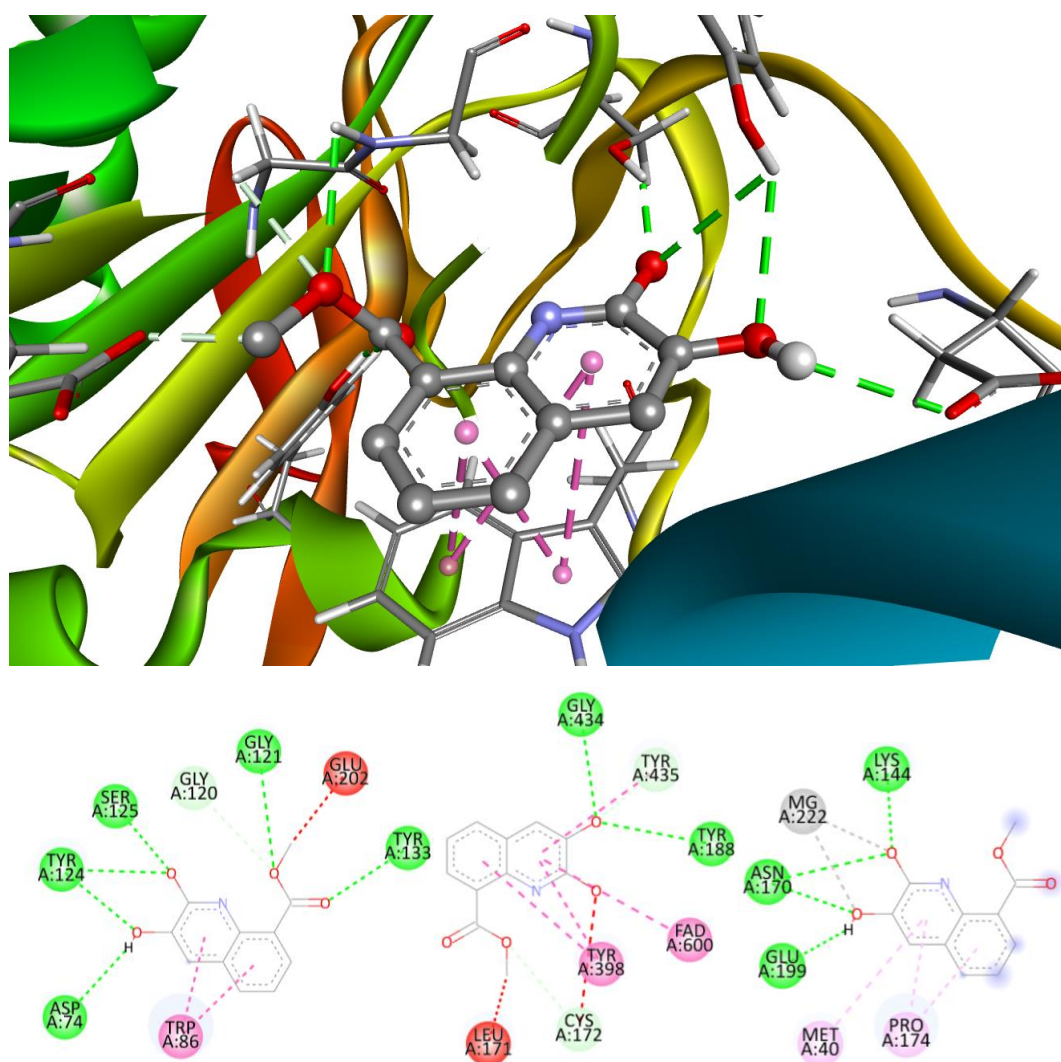


**Figure 7.** 3D representation of the interactions between dQ829 and the AChE (Top). Bottom: 2D interaction map for the complexes of the quinoline analog with AChE (left), MAOB (middle) and COMT (right). H-bonds are represented in green color, non-conventional C-H bonds are in green light, metal-donor are in gray,  $\pi$ -interactions are in pink and purple, and steric effects are in red.

Finally, the interaction between the active site of COMT and dQ829 is presented in the bottom-right corner of the Figure 8. In this case, the catechol group are the responsible for the stabilization of the adduct. There are several examples in the literature that indicate the inhibition the dopamine degradation by catechol-type compounds [107], in fact Tolcapone is nitro-catechol compound used as therapeutic drug against Parkinson disease. Interestingly the interaction form between the quinoline analog and the Tolcapone with COMT is very similar in several ways. Both compounds present two metal-donor interactions between the  $Mg^{II}$  ion and the catechol moiety. These same oxygen atoms forms H-bonds with Lys144, Asn170 and Glu199. The difference arises from the number of H-bonds that each residue can forms whereas tolcapone forms two of these interactions with Glu199 (deprotonated residue), whereas dQ829 makes them the same with Asn170 (neutral residue). Other marked difference is the stabilization provided by the nitro group in Tolcapone that lacks in the quinoline derivative. These last unions seem to make a difference in terms of the stability of the complexes formed, with tolcapone having a higher affinity for COMT than the dQ829 compound. Nevertheless, we must not lose sight that, according to the results of the simulations, this functionalized quinoline has significant neuroprotective activity. Although various catechol compounds were tested, none performed as well as dQ829, the origin of that remains unclear.

Docking simulations indicate that some compounds present high performance in the inhibition of MAO-B and AChE proteins as Tacrine does. In this context, six quinoline derivatives are presented as promising candidates to act against AD and anxiety disorders. According with the results in COMT enzyme, dQ829 is a hopeful molecule to be investigated against PD.

In further studies, it is expected to evaluate the neuroprotective and antioxidant capacity of this quinoline derivatives with more accurately simulations and in a middle-time try to synthesize the most promising compounds in biological tests.

#### 4. Conclusions

Quinoline derivatives represent a privileged molecular scaffold to build derivatives with interesting biological activities. In this sense, the response to two of the most severe problems faced by adults and national health systems, AD and PD, may come from one of these derivatives.

In this work we have created and analyzed a chemical space containing 8356 derivatives adding -OH, -SH, -NH<sub>2</sub>, -COH, -COCH<sub>3</sub> and -COOCH<sub>3</sub> to quinoline framework. The compounds were sampling and analyzed using the CADMA-Chem protocol based on the chemical properties of the compounds to find the most promising candidates as antioxidant and at the same time, neuroprotective agents.

Through the selection ( $S^S$ ) and elimination scores ( $S^E$ ), the group was reduced to 25 compounds, which according to the results obtained, would present less toxicity, improved bioavailability, and easy manufacturability, all these properties represent advantages for the oral drugs production.

According to eH-DAMA outcomes, dQ49, dQ829, dQ950, dQ1356, dQ1368, dQ2355 and dQ2357 derivatives have the most promising scavenging capability. The enhanced radical scavenging efficiency compared with the reference antioxidants Trolox and  $\alpha$ -tocopherol, would come from simple electron transfer (SET) and hydrogen atom transfer (HAT) mechanisms. However, these compounds present a less scavenging activity than ascorbate ion in SET mechanisms but a better antioxidant behavior via HAT process.

On the other hand, the coupling simulations indicate that quinoline only presents neuroprotective activity on the MAOB enzyme. Some of its derivatives can act as inhibitors of this enzyme and the AChE protein. The most efficient compounds for this purpose are dQ49, dQ815, dQ829, dQ954, dQ1368 and dQ2357. Additionally, the derivative dQ829 might have activity by inhibiting the COMT protein by binding in a very similar way like Tolcapone, a drug used to treat PD, does. Evidence of some structural details that favor neuroprotective activity was found. Compounds with amino groups do not favor the neuroprotective activity of dopamine, while, to some extent, catechol groups can enhance it, also, aldehyde and ester groups improve the affinity of the compounds for the AChE enzyme. These insights could be used in future design protocols.

Considering the data obtained as a whole, it is the derivatives dQ49, dQ829, dQ8368 and dQ2357 that represent the best candidates for future research. At least the dQ829 compound certainly they deserve further analysis on their role as neuroprotectors.

**Supplementary Materials:** The following supporting information can be downloaded at: [www.mdpi.com/xxx/s1](http://www.mdpi.com/xxx/s1), Table S1. Properties determined to the Quinoline derivatives, Table S2. ADME, toxicity and synthetic accessibility of the reference set Figure S1. Deprotonation paths and pK<sub>a</sub> values for the 25 most promising dQ. Table S3. Ionization energy and bond dissociation energy of quinoline derivatives and Table S4. Complete set of docking values.

**Author Contributions:** Conceptualization, A.G.; Investigation, E.G.G-G., L.F.H-A.; Formal Analysis, L.F.H-A. and A.G.; Methodology, E.G.G-G., L.F.H-A. and A.G.; Project Administration, A.G.; Supervision, A.G.; Validation, E.G.G-G., L.F.H-A.; Visualization, E.G.G-G., L.F.H-A. and A.G.; Writing – Original Draft Preparation, E.G.G-G., M.R., L.F.H-A.; Writing – Review & Editing, A.G.

**Acknowledgments:** L.F.H.A thanks to Estancias Posdoctorales por México (2022) CONACyT program for postdoctoral grant.. We gratefully thank to the Laboratorio de Visualización y Cómputo Paralelo at Universidad Autónoma Metropolitana-Iztapalapa for computing time. E.G.G.L. acknowledges CONACyT for Doctoral fellowship.

**Conflicts of Interest:** The authors declare no conflicts of interest.

## References

1. Sies, H. Oxidative Stress: Concept and Some Practical Aspects. *Antioxidants* 2020, 9, 852.
2. Hajam, Y.A.; Rani, R.; Ganie, S.Y.; Sheikh, T.A.; Javaid, D.; Qadri, S.S.; Pramodh, S.; Alsulimani, A.; Alkhanani, M.F.; Harakeh, S.; Arif, H.; Haque S.; Reshi, M. S. Oxidative Stress in Human Pathology and Aging: Molecular Mechanisms and Perspectives. *Cells* 2022, 11, 552.
3. Vona, R.; Pallotta, L.; Cappelletti, M.; Severi, C.; Matarrese, P. The Impact of Oxidative Stress in Human Pathology: Focus on Gastrointestinal Disorders. *Antioxidants* 2021, 10, 201.
4. Masschelin P. M.; Cox A. R.; Chernis Natasha, Hartig Sean M. The Impact of Oxidative Stress on Adipose Tissue Energy Balance. *Front. Phys.* 2020, 10.
5. Chen, Y.; Qin, C. ; Huang, J. ; Tang, X.; Liu, C.; Huang, K.; Xu, K.; Guo, G.; Tong, A.; Zhou, L. The role of astrocytes in oxidative stress of central nervous system: A mixed blessing. *Cell. Prolif.* 2020; 53:e12781.
6. Kuresh, A. Y.; Martin, A.; Joseph, J. A. Essential fatty acids and the brain: possible health implications, *Int. J. Dev. Neurosci.* 2000, 18, 4-5, 338-399.
7. Lee, C. S.; Leong, K. W. Advances in microphysiological blood-brain barrier (BBB) models towards drug delivery, *Current Opinion in Biotechnology*, 2020, 66, 78-87,
8. Bang, S.; Lee, SR.; Ko, J.; Son, K.; Tahk, D.; Ahn, J.; Im, I.; Jeon, N. L. A Low Permeability Microfluidic Blood-Brain Barrier Platform with Direct Contact between Perfusable Vascular Network and Astrocytes. *Sci. Rep.* 2017, 7, 8083.
9. Franke, H.; Galla, H. J.; Beuckmann, C. T.; An improved low-permeability in vitro-model of the blood–brain barrier: transport studies on retinoids, sucrose, haloperidol, caffeine and mannitol, *Brain Res.*, 1999, 818, 1, 65-71.
10. Rekatsina, M. ; Paladini, A. ; Pirolì, A. ; Zis, P.; Pergolizzi, J. V. ; Varrassi, G. Pathophysiology and Therapeutic Perspectives of Oxidative Stress and Neurodegenerative Diseases: A Narrative Review. *Adv. Ther.* 2020, 37, 113–139.
11. Konovalova, J.; Gerasymchuk, D.; Parkkinen, I.; Chmielarz, P.; Domanskyi, A. Interplay between MicroRNAs and Oxidative Stress in Neurodegenerative Diseases. *Int. J. Mol. Sci.* 2019, 20, 6055.
12. Bhatt, S.; Puli, L.; Patil, C. R. Role of reactive oxygen species in the progression of Alzheimer's disease. *Drug Discov. Today* 2021,26, 3, 794-803.
13. Zuo, L.; Motherwell, M. S. The impact of reactive oxygen species and genetic mitochondrial mutations in Parkinson's disease. *Gene* 2013, 532, 1, 2013, 18-23.
14. Bai, R.; Guo, J.; Ye, X., Xie, Y.; Xie, T. Oxidative stress: The core pathogenesis and mechanism of Alzheimer's disease. *Ageing Res. Rev.* 2022, 77, 1568-1637.
15. Juszczak, G.; Mikulska, J.; Kasperek, K.; Pietrzak, D.; Mrozek, W.; Herbet, M. Chronic Stress and Oxidative Stress as Common Factors of the Pathogenesis of Depression and Alzheimer's Disease: The Role of Antioxidants in Prevention and Treatment. *Antioxidants* 2021, 10, 1439.
16. Sayre, L. M.; Smith, M. A., Perry G. Chemistry and biochemistry of oxidative stress in neurodegenerative disease. *Curr Med. Chem.* 2001, 8, 721-38.
17. De Leo M. E.; Borrello, S.; Passantino, M.; Palazzotti B.; Mordente, A.; Daniele, A. Oxidative stress and overexpression of manganese superoxide dismutase in patients with Alzheimer's disease. *Neurosci. Lett.* 1998, 250, 3, 173-176.
18. Dhib-Jalbut, S; Arnold, D. L., Cleveland D. W.; Fisher, M.; Friedlander, M.; Mouradian, M. M.. Neurodegeneration and neuroprotection in multiple sclerosis and other neurodegenerative diseases. *J. Neuroimmunol.* 2006, 176, 1-2, 198-215.
19. Cai, Z.; Zhao, B.; Ratka, A. Oxidative Stress and  $\beta$ -Amyloid Protein in Alzheimer's Disease. *Neuromol. Med.* 2011, 13, 223–250.
20. Butterfield, D. A.; Lauderback, C. M.; Lipid peroxidation and protein oxidation in Alzheimer's disease brain: potential causes and consequences involving amyloid  $\beta$ -peptide-associated free radical oxidative stress. *Free Rad. Biol. Med.* 2002, 32, 11, 1050-1060.
21. Chen, L; Fan, Y.; Zhao, L.; Zhang, Q.; Wang Z. The metal ion hypothesis of Alzheimer's disease and the anti-neuroinflammatory effect of metal chelators, *Bioorg. Chem.*,2023, 131, 106301.
22. Everett, J.; Lermite, F.; Brooks, J.; Tjendana-Tjhin, V.; Plascencia-Villa, G.; Hands-Portman, I.; Donnelly, J. M.; Billimoria, K.; Perry, G.; Zhu, X.; Sadler, P. J.; O'Connor, P. B.; Collingwood, J. F.; Telling, N. D. Biogenic metallic elements in the human brain? *Sci. Adv.* 2021, 7, eabf6707.
23. Das, N.; Raymick, J.; Sarkar, S. Role of metals in Alzheimer's disease. *Metab. Brain. Dis.* 2021, 36, 1627–1639.
24. Brewer, G. J. Iron and Copper Toxicity in Diseases of Aging, Particularly Atherosclerosis and Alzheimer's Disease. *Exp. Biol. Med.* 2007, 232, 2, 323-335.

25. Perry, G.; Taddeo, M.A.; Petersen, R.B.; Castellani, R. J.; Harris, P. L. R.; Siedlak, S. L.; Cash, A. D.; Liu, Q.; Nunomura, A.; Atwood, C. S.; Smith, M. A. Adventitiously-bound redox active iron and copper are at the center of oxidative damage in Alzheimer disease. *Biomaterials* 2003, 16, 77–81.
26. Chen, C.; Turnbull, D.M.; Reeve, A.K. Mitochondrial Dysfunction in Parkinson's Disease—Cause or Consequence? *Biology* 2019, 8, 38.
27. Tatton, W.G.; Chalmers-Redman, R.; Brown, D.; Tatton, N. Apoptosis in Parkinson's disease: Signals for neuronal degradation. *Ann. Neurol.*, 2003, 53, S61–S72.
28. Jenner, P. Oxidative stress in Parkinson's disease. *Ann Neurol.* 2003 53: S26–S38.
29. Pajares, M.; I. Rojo, A.; Manda, G.; Boscá, L.; Cuadrado, A. Inflammation in Parkinson's Disease: Mechanisms and Therapeutic Implications. *Cells* 2020, 9, 1687.
30. Nunes, C. Laranjinha, J.; Nitric oxide and dopamine metabolism converge via mitochondrial dysfunction in the mechanisms of neurodegeneration in Parkinson's disease, *Archives of Biochemistry and Biophysics*, 2021, 704, 108877.
31. Sun, Y.; Pham, A.N.; Waite, T.D. Elucidation of the interplay between Fe(II), Fe(III), and dopamine with relevance to iron solubilization and reactive oxygen species generation by catecholamines. *J. Neurochem.* 2016, 137, 955–968.
32. Meiser, J.; Weindl, D.; Hiller, K. Complexity of dopamine metabolism. *Cell. Commun. Signal.* 2013, 11, 34.
33. Forsberg, M.M.; Juvonen, R.O.; Helisalmi, P.; Leppänen, J.; Gogos, J. A.; Karayiorgou, M.; Männistö, P. T. Lack of increased oxidative stress in catechol-O-methyltransferase (COMT)-deficient mice. *Naunyn-Schmiedeberg's Arch. Pharmacol.* 2004, 370, 279–289.
34. Delcambre, S.; Nonnenmacher, Y.; Hiller, K. Dopamine Metabolism and Reactive Oxygen Species Production. In: Buhlman, L. (eds) *Mitochondrial Mechanisms of Degeneration and Repair in Parkinson's Disease*. Springer, Cham.
35. Iuga C.; Alvarez-Idaboy, J. R.; Vivier-Bunge, A. ROS initiated oxidation of dopamine under oxidative stress conditions in aqueous and lipidic environments. *J. Phys. Chem. B.* 2011, 115(42), 12234–12246.
36. Chauhan, M.S.S.; Umar, T.; Aulakh, M. K. Quinolines: Privileged Scaffolds for Developing New Anti-neurodegenerative Agents *Chem. Select* 2023, 8, e202204960.
37. Yadav, V.; Reang, J.; Sharma, V.; Majeed, J.; Sharma, P. C. Sharma; K., Giri, N.; Kumar, A.; Tonk, R. K. Quinoline-derivatives as privileged scaffolds for medicinal and pharmaceutical chemists: A comprehensive review. *Chem. Biol. Drug Des.* 2022, 100, 389–418.
38. Musiol, R. An overview of quinoline as a privileged scaffold in cancer drug discovery. *Expert Opin Drug Disco*, 2017 12, 6, 583–597,
39. Bongarzone, S.; Bolognesi, M. L. The concept of privileged structures in rational drug design: focus on acridine and quinoline scaffolds in neurodegenerative and protozoan diseases, *Expert Opin. Drug Discov.* 2011 6:3, 251–268.
40. Yadav, P.; Shah, K. Quinolines, a perpetual, multipurpose scaffold in medicinal chemistry. *Bioorg. Chem.*, 2021, 109, 104639.
41. Almansour, A.I.; Arumugam, N.; Prasad, S.; Kumar, R.S.; Alsalihi, M.S.; Alkaltham, M.F.; Al-Tamimi, H.b.A. Investigation of the Optical Properties of a Novel Class of Quinoline Derivatives and Their Random Laser Properties Using ZnO Nanoparticles. *Molecules* 2022, 27, 145.
42. Lewinska, G.; Sanetra, J.; Marszałek, K.W. Application of quinoline derivatives in third-generation photovoltaics. *J. Mater. Sci.: Mater. Electron* 2021, 32, 18451–18465.
43. Aygün, B.; Alaylar, B.; Turhan, K.; Şakar, E.; Karadayı, M.; Abu Al-Sayyed, M. I.; Pelit, E.; Güllüce, M.; Karabulut, A.; Turgut, Z.; Alım, Investigation of neutron and gamma radiation protective characteristics of synthesized quinoline derivatives. *Int. J. Rad. Biol.* 2020, 96, 11, 1423–1434.
44. Gentile, D.; Fuochi, V.; Rescifina, A.; Furneri, P.M. New Anti SARS-Cov-2 Targets for Quinoline Derivatives Chloroquine and Hydroxychloroquine. *Int. J. Mol. Sci.* 2020, 21, 5856.
45. Achan, J.; Talisuna, A.O.; Erhart, A.; Yeka, A.; Tibenderana, J. K.; Baliraine, F. N.; Rosenthal, P. J.; D'Alessandro, U. Quinine, an old anti-malarial drug in a modern world: role in the treatment of malaria. *Malar. J.* 2011, 10, 144.
46. Shang, X. F.; Morris-Natschke, S. L.; Yang, G. Z.; Liu, Y. Q.; Guo, X.; Xu, X. S.; Goto, M.; Li, J. C.; Zhang, J.; Lee, H. S. Biologically active quinoline and quinazoline alkaloids part II. *Med. Res. Rev.* 2018, 38, 1614–1660
47. Summers K. L.; Roseman, G. P.; Sopasis, G. J.; Millhauser, G. L.; Harris, H. H.; Pickering, I. J.; George, G. N. Copper(II) Binding to PBT2 Differs from That of Other 8-Hydroxyquinoline Chelators: Implications for the Treatment of Neurodegenerative Protein Misfolding Diseases *Inorg. Chem.* 2020, 59, 23, 17519–17534
48. Bains, A. K.; Singh, V.; Adhikari, D. Homogeneous nickel-catalyzed sustainable synthesis of quinoline and quinoxaline under aerobic conditions. *J. Org. Chem.* 2020 85(23), 14971–14979.
49. El-Saghier, A. M.; El-Naggar, M.; Hussein Abdel, H. M.; El-Adasy, A. B.; A., Olish, M.; Abdelmonsef, A. H. Eco-Friendly Synthesis, Biological Evaluation, and In Silico Molecular Docking Approach of Some New Quinoline Derivatives as Potential Antioxidant and Antibacterial Agents. *Front. Chem.*, 2020, 9. <https://doi.org/10.3389/fchem.2021.679967>
50. Patel, A.; Patel, S.; Mehta, M.; Patel, Y.; Patel R.; Shah, D.; Patel, D.; Shah, D.; Patel, M.; Patel, M.; Solanki, N.; Bambharoliya, T.; Patel, S.; Nagani, A.; Patel, H.; Vaghasiya, J.; Shah, H.; Prajapati, H.; Rathod, M.; Bhimani, B.; Patel, R.; Bhavsar, R.; Rakholiya, B.; Patel, M.; Patel, P. A review on synthetic investigation for quinoline- recent green approaches, *Green Chem. Lett. Rev.* 2022, 15, 2, 337–372.
51. Jaiswal, A.; Sharma, A. K.; Jaiswal, S.; Mishra, A.; Singh, J.; Singh, J.; Siddiqui, I. R. J. *Heterocycl. Chem.* 2023, 60, 7, 1122.



52. Harikrishna, S.; Gangu K. K.; Robert, A. R.; Ganja, H.; Kerru, M.; Maddila, S.; Jonnalagadda, S. B. An ecofriendly and reusable catalyst RuO<sub>2</sub>/MWCNT in the green synthesis of sulfonyl-quinolines, *PSEP*, 2022, 159, 99–117. 539
53. Matada, B. S.; Pattanashettar, R.; Yernale, N. G. A comprehensive review on the biological interest of quinoline and its derivatives. *Bioorg. Med. Chem.* 2021, 32, 115973. 540
54. Dib, M.; Ouchetto, H.; Ouchetto, K.; Hafid, A.; Khouili, M. Recent developments of quinoline derivatives and their potential biological activities. *Curr. Org. Synth.*, 2022, 18, 3, 248–269. 541
55. Chu, X. M.; Wang, C.; Liu, W.; Liang, L. L.; Gong, K. K.; Zhao, C. Y.; Sun, K. L. Quinoline and quinolone dimers and their biological activities: An overview. *Eur. J. Med. Chem.*, 2019, 161, 101–117. 542
56. Kumari, L.; Mazumder, A.; Pandey, D.; Yar, M. S.; Kumar, R.; Mazumder, R.; Gupta, S. Synthesis and biological potentials of quinoline analogues: A review of literature. *Mini Rev. Org. Chem.*, 2019, 16, 7, 653–688. 543
57. Loiseau, P.M.; Balaraman, K.; Barratt, G.; Pomel, S.; Durand, R.; Frézard, F.; Figadère, B. The Potential of 2-Substituted Quinolines as Antileishmanial Drug Candidates. *Molecules* 2022, 27, 2313. 544
58. Kucharski, D.J.; Jaszczak, M.K.; Boratyński, P.J. A Review of Modifications of Quinoline Antimalarials: Mefloquine and (hydroxy)Chloroquine. *Molecules* 2022, 27, 1003. 545
59. Zeleke, D.; Eswaramoorthy, R.; Belay, Z.; Melaku, Y. Synthesis and antibacterial, antioxidant, and molecular docking analysis of some novel quinoline derivatives. *J. Chem.* 2020. 1–16. 546
60. Moor, L. F.; Vasconcelos, T. R.; da R Reis, R.; Pinto, L. S., & da Costa, T. M. Quinoline: an attractive scaffold in drug design. *Mini Rev. Med. Chem.*, 2021, 21, 16, 2209–2226. 547
61. Tran, T.N.; Henary, M. Synthesis and Applications of Nitrogen-Containing Heterocycles as Antiviral Agents. *Molecules* 2022, 27, 2700. 548
62. Teixeira, M.M.; Carvalho, D.T.; Sousa, E.; Pinto, E. New Antifungal Agents with Azole Moieties. *Pharmaceuticals* 2022, 15, 1427. 549
63. Katariya, K. D.; Shah, S.R.; Reddy, S.R. Anticancer, antimicrobial activities of quinoline based hydrazone analogues: Synthesis, characterization and molecular docking. *Bioorg. Chem.* 2020, 94, 103406. 550
64. Eissa, S. I.; Farrag, A. M.; Abbas, S. Y.; El Shehry, M. F.; Ragab, A.; Fayed, E. A. Novel structural hybrids of quinoline and thiazole moieties: Synthesis and evaluation of antibacterial and antifungal activities with molecular modeling studies. *Bioorg. Chem.* 2021, 110, 104803. 551
65. Douadi, K.; Chafaa, S.; Douadi, T.; Al-Noaimi, M.; Kaabi, I. Azoimine quinoline derivatives: Synthesis, classical and electrochemical evaluation of antioxidant, anti-inflammatory, antimicrobial activities and the DNA/BSA binding. *J. Mol. Struct.* 2020, 1217, 128305. 552
66. Amariuca-Mantu, D.; Mangalagiu, V.; Bejan, I.; Aricu, A.; Mangalagiu, I.I. Hybrid Azine Derivatives: A Useful Approach for Antimicrobial Therapy. *Pharmaceutics* 2022, 14, 2026. 553
67. Kalita, J.; Chetia, D.; Rudrapal, M. Design, synthesis, antimalarial activity and docking study of 7-chloro-4-(2-(substituted benzylidene)hydrazineyl)quinolines. *J. Med. Chem. Drug Des.* 2019, 2, 1, 928–937. 554
68. Abdelbaset, M. S.; Abdel-Aziz, M.; Abuo-Rahma, G. E. D. A.; Abdelrahman, M. H.; Ramadan, M.; Youssif, B. G. M. Novel quinoline derivatives carrying nitrones/oximes nitric oxide donors: Design, synthesis, antiproliferative and caspase-3 activation activities. *Arch. Pharm.* 2018. 352, 1, 1800270. 555
69. Rani, A.; Sharma, A.; Legac, J.; Rosenthal, P. J.; Singh, P.; Kumar, V. A trio of quinoline-isoniazid-phthalimide with promising antiplasmodial potential: Synthesis, invitro evaluation and heme-polymerization inhibition studies. *Bioorg. Med. Chem.* 2021 39, 116159. 556
70. Ebenezer, O.; Jordaan, M.A.; Carena, G.; Bono, T.; Shapi, M.; Tuszyński, J.A. An Overview of the Biological Evaluation of Selected Nitrogen-Containing Heterocycle Medicinal Chemistry Compounds. *Int. J. Mol. Sci.* 2022, 23, 8117. 557
71. Guzman-Lopez, E.G.; Reina, M.; Perez-Gonzalez, A.; Francisco-Marquez, M.; Hernandez-Ayala, L.F.; Castañeda-Arriaga, R.; Galano, A. CADMA-Chem: A Computational Protocol Based on Chemical Properties Aimed to Design Multifunctional Antioxidants. *Int. J. Mol. Sci.* 2022, 23, 13246. 558
72. RDKit: Open-source cheminformatics. <https://www.rdkit.org> 559
73. Lipinski, C.A.; Lombardo, F.; Dominy, B.W.; Feeney, P.J. Experimental and computational approaches to estimate solubility and permeability in drug discovery and development settings. *Adv. Drug. Deliv. Rev.* 2001, 46, 3–26. 560
74. Ghose, A.K.; Viswanadhan, V.N.; Wendoloski, J.J. A Knowledge-Based Approach in Designing Combinatorial or Medicinal Chemistry Libraries for Drug Discovery. 1. A Qualitative and Quantitative Characterization of Known Drug Databases. *J. Comb. Chem.* 1999, 1, 55–68. 561
75. Veber, D.F.; Johnson, S.R.; Cheng, H.Y.; Smith, B.R.; Ward, K.W.; Kopple, K.D. Molecular Properties That Influence the Oral Bioavailability of Drug Candidates. *J. Med. Chem.* 2002, 45, 2615–2623. 562
76. Egan, W. J.; Merz, K. M. Jr.; Baldwin, J. J. Prediction of drug absorption using multivariate statistics. *J. Med. Chem.* 2000, 43, 21, 3867–3877. 563
77. Muegge, I.; Heald, S.L.; Brittelli, D. Simple selection criteria for drug-like chemical matter. *J. Med. Chem.* 2001, 44, 12, 1841–6. 564
78. Kochev, N.; Avramova, S.; Angelov, P.; Jeliaskova, N. Computational Prediction of Synthetic Accessibility of Organic Molecules with Ambit-Synthetic Accessibility Tool. *Org. Chem. Ind. J.* 2018, 14, 2, 123. 565
79. Martin, T. Toxicity Estimation Software Tool (TEST). U.S. Environmental Protection Agency, Washington, DC, 2016. 566
80. Reina, M.; Castañeda-Arriaga, R.; Pérez-González, A.; Guzman-Lopez, E.; Tan, D.-X.; Reiter, R.; Galano, A. A Computer-Assisted Systematic Search for Melatonin Derivatives with High Potential as Antioxidants. *Melatonin Res.* 2018, 1, 27–58. 567



81. Zhong H.A.; Mashinson, V.; Woolman T. A.; Zha M. Understanding the molecular properties and metabolism of top prescribed drugs. *Curr. Top. Med. Chem.* 2013, 13, 11, 1290–1307. 599
82. Gaussian 16, Revision C.01, Frisch, M. J.; Trucks, G. W.; Schlegel, H. B.; Scuseria, G. E.; Robb, M. A.; Cheeseman, J. R.; Scalmani, G.; Barone, V.; Petersson, G. A.; Nakatsuji, H.; Li, X.; Caricato, M.; Marenich, A. V.; Bloino, J.; Janesko, B. G.; Gomperts, R.; Mennucci, B.; Hratchian, H. P.; Ortiz, J. V.; Izmaylov, A. F.; Sonnenberg, J. L.; Williams-Young, D.; Ding, F.; Lipparini, F.; Egidi, F.; Goings, J.; Peng, B.; Petrone, A.; Henderson, T.; Ranasinghe, D.; Zakrzewski, V. G.; Gao, J.; Rega, N.; Zheng, G.; Liang, W.; Hada, M.; Ehara, M.; Toyota, K.; Fukuda, R.; Hasegawa, J.; Ishida, M.; Nakajima, T.; Honda, Y.; Kitao, O.; Nakai, H.; Vreven, T.; Throssell, K.; Montgomery, J. A., Jr.; Peralta, J. E.; Ogliaro, F.; Bearpark, M. J.; Heyd, J. J.; Brothers, E. N.; Kudin, K. N.; Staroverov, V. N.; Keith, T. A.; Kobayashi, R.; Normand, J.; Raghavachari, K.; Rendell, A. P.; Burant, J. C.; Iyengar, S. S.; Tomasi, J.; Cossi, M.; Millam, J. M.; Klene, M.; Adamo, C.; Cammi, R.; Ochterski, J. W.; Martin, R. L.; Morokuma, K.; Farkas, O.; Foresman, J. B.; Fox, D. J. Gaussian, Inc., Wallingford CT, 2016. 600
83. Marenich, A.V.; Cramer, C.J.; Truhlar, D.G. Universal solvation model based on solute electron density and on a continuum model of the solvent defined by the bulk dielectric constant and atomic surface tensions. *J. Phys. Chem. B* 2009, 113, 6378–6396. 601
84. Zhao, Y.; Schultz, N.E.; Truhlar, D.G. Design of Density Functionals by Combining the Method of Constraint Satisfaction with Parametrization for Thermochemistry, Thermochemical Kinetics, and Noncovalent Interactions. *J. Chem. Theory Comput.* 2006, 2, 364–382. 602
85. Castro-González, L.M.; Alvarez-Idaboy, J.R.; Galano, A. Computationally Designed Sesamol Derivatives Proposed as Potent Antioxidants. *ACS Omega* 2020, 5, 9566–9575. 603
86. Pérez-González, A.; Castañeda-Arriaga, R.; Guzmán-López, E.G.; Hernández-Ayala, L.F.; Galano, A. Chalcone Derivatives with a High Potential as Multifunctional Antioxidant Neuroprotectors. *ACS Omega* 2022, 7, 38254–38268. 604
87. Reina, M.; Guzmán-López, E.G.; Romeo, I.; Marino, T.; Russo, N.; Galano, A. Computationally designed: P -coumaric acid analogs: Searching for neuroprotective antioxidants. *New J. Chem.* 2021, 45, 14369–14380. 605
88. Galano, A. On the direct scavenging activity of melatonin towards hydroxyl and a series of peroxy radicals. *Phys. Chem. Chem. Phys.* 2011, 13, 7178–7188. 606
89. Galano, A.; Alvarez-Idaboy, J.R.; Francisco-Márquez, M. Physicochemical Insights on the Free Radical Scavenging Activity of Sesamol: Importance of the Acid/Base Equilibrium. *J. Phys. Chem. B* 2011, 115, 13101–13109. 607
90. Ortiz, J.V. Electron propagator theory: An approach to prediction and interpretation in quantum chemistry. *Wiley Interdiscip. Rev.: Comput. Mol. Sci.* 2013, 3, 123–142. 608
91. Marvin 23.8.0, 2023, ChemAxon (<http://www.chemaxon.com>). 609
92. Galano, A.; Pérez-González, A.; Castañeda-Arriaga, R.; Muñoz-Rugeles, L.; Mendoza-Sarmiento, G.; Romero-Silva, A.; Ibarra-Escutia, A.; Rebollar-Zepeda, A.M.; León-Carmona, J.R.; Hernández-Olivares, M.A.; et al. Empirically Fitted Parameters for Calculating pKa Values with Small Deviations from Experiments Using a Simple Computational Strategy. *J. Chem. Inf. Model.* 2016, 56, 1714–1724. 610
93. Guzmán-López, E.G.; Reina, M.; Hernández-Ayala, L.F.; Galano, A. Rational Design of Multifunctional Ferulic Acid Derivatives Aimed for Alzheimer's and Parkinson's Diseases. *Antioxidants* 2023, 12, 1256. 611
94. Ellermann, M.; Lerner, C.; Burgy, G.; Ehler, A.; Bissantz, C.; Jakob-Roetne, R.; Paulini, R.; Allemann, O.; Tissot, H.; Grünstein, D.; et al. Catechol-O-methyltransferase in complex with substituted 3'-deoxyribose bisubstrate inhibitors. *Acta Crystallogr. Sect. D. Biol. Crystallogr.* 2012, 68, 253–260. 612
95. Binda, C.; Wang, J.; Pisani, L.; Caccia, C.; Carotti, A.; Salvati, P.; Edmondson, D.E.; Mattevi, A. Structures of human monoamine oxidase B complexes with selective noncovalent inhibitors: Saffinamide and coumarin analogs. *J. Med. Chem.* 2007, 50, 5848–5852. 613
96. Cheung, J.; Rudolph, M.J.; Burshteyn, F.; Cassidy, M.S.; Gary, E.N.; Love, J.; Franklin, M.C.; Height, J.J. Structures of human acetylcholinesterase in complex with pharmacologically important ligands. *J. Med. Chem.* 2012, 55, 10282–10286. 614
97. Webb, B.; Sali, A. Comparative Protein Structure Modeling Using Modeller. *Current Protocols in Bioinformatics*, John Wiley & Sons, Inc., 5.6.1–5.6.37, 2016. 615
98. Morris, G. M.; Huey, R.; Lindstrom, W.; Sanner, M. F.; Belew, R. K.; Goodsell, D. S.; Olson, A. J. Autodock4 and AutoDockTools4: automated docking with selective receptor flexibility. *J. Comput. Chem.* 2009, 30, 16, 2785–91. 616
99. Eberhardt, J.; Santos-Martins, D.; Tillack, A. F.; Forli, S. AutoDock Vina 1.2.0: New Docking Methods, Expanded Force Field, and Python Bindings. *J. Chem. Inf. Model.* 2021, 61, 8, 3891–3898. 617
100. BIOVIA, Dassault Systèmes, Discovery Studio 2021 Client, San Diego: Dassault Systèmes, 2023. 618
101. Learmonth, D.A.; Bonifácio, M.J.; Soares-da-Silva, P. Synthesis and Biological Evaluation of a Novel Series of “Ortho-Nitrated” Inhibitors of Catechol-O-methyltransferase. *J. Med. Chem.* 2005, 48, 8070–8078. 619
102. A. Bendich, L.J. Machlin, O. Scandurra, G.W. Burton, D.D.M. Wayner, The antioxidant role of vitamin C, *Adv. Free Rad. Biol. Med.*, 1986, 2, 2, 419–444. 620
103. Silman, I.; Sussman J.L.; Acetylcholinesterase: how is structure related to function? *Chem. Biol. Interact.* 2008, 175, 1–3, 3–10. 621
104. Harel, M.; Schalk, I.; Ehret-Sabatier, L.; Bouet, F.; Goeldner, M.; Hirth, C.; Axelsen, P.H.; Silman, I.; Sussman, J.L.; Quaternary ligand binding to aromatic residues in the active-site gorge of acetylcholinesterase. *Proc. Natl. Acad. Sci. U.S.A.* 1993, 90, 19, 9031–9035. 622
105. Ma, J.; Ito A. Tyrosine residues near the FAD binding site are critical for FAD binding and for the maintenance of the stable and active conformation of rat monoamine oxidase. *J. Biochem.* 2002, 131, 1, 107–11. 623

- 
106. Edmondson, D.E.; Binda, C.; Mattevi, A. The FAD binding sites of human monoamine oxidases A and B. *Neurotoxicology* 2004, 25, 1-2, 63-72. 658  
659
107. Kiss, L.E.; Soares-Da-Silva, P. Medicinal chemistry of catechol O -methyltransferase (COMT) inhibitors and their therapeutic utility. *J. Med. Chem.* 2014, 57, 8692–8717. 660  
661  
662